Mon. Not. R. astr. Soc. (1969) **145**, 297–308.

THE EMITTED SPECTRUM OF A PROTO-STAR

Richard B. Larson

(Communicated by P. Demarque)

(Received 1969 February 4)

SUMMARY

The spectral energy distribution emitted by a collapsing proto-star has been calculated on the basis of some simple approximations for the radiative transfer in the extended spherical 'atmosphere' of the proto-star. Results for the evolution in spectral appearance are presented for several of the collapsing proto-star calculations described in a previous paper (Larson 1969). Comparison is made with some observations of infra-red objects in Orion and with recent infra-red observations of T Tauri stars.

1. INTRODUCTION

In a previous paper (Larson 1969, hereafter referred to as Paper I), we have described the results of some numerical calculations of the dynamics of a spherically symmetric collapsing proto-star. It was found that during most of its evolution a proto-star consists of a small central core or 'embryo star' surrounded by an extended optically thick cloud of infalling material. The energy radiated from the stellar core is absorbed by the dust grains in the infalling material, and re-emitted thermally as infra-red wavelengths; thus the proto-star appears during most of its evolution as an infra-red object. In this paper we consider the radiation transfer in the infalling cloud, with the purpose of calculating the emitted spectrum.

Since the radiation is emitted from a very extended region, it is essential to take the spherical geometry into account; the theory of plane-parallel atmospheres cannot be applied. The little work that has previously been done on radiation transfer in extended spherical atmospheres (see for example Chapman 1966) has referred only to rather special cases and has, in any case, not been directed toward calculating the emitted spectrum. In this paper we consider a simple model for the extended spherical 'atmosphere' of a proto-star, based on the following assumptions:

(1) The product of the opacity κ_λ and the density ρ is assumed to vary with radius according to an inverse power law of the form

$$\kappa_\lambda \rho = K_\lambda r^{-n}. \tag{1}$$

It is found in the dynamical calculations (Paper I) that ρ is closely proportional to $r^{-3/2}$ throughout almost the entire region important for the radiative transfer problem; thus if we take $n = 3/2$, equation (1) is in fact a good assumption, provided that the dust absorption properties do not vary with r.

(2) In the absence of any knowledge of the dust absorption coefficient at the relevant high temperatures and infra-red wavelengths, the following simple law has been assumed:

$$\kappa_\lambda = \kappa_0 \lambda^{-p}, \tag{2}$$

where κ_0 and p are regarded as free parameters. The data of Johnson & Borgmann (1963) and Johnson (1965) on the wavelength dependence of the interstellar extinction at near infra-red wavelengths are roughly represented by the law $\kappa_\lambda \propto \lambda^{-3/2}$; however, these data are not necessarily of any relevance to the present problem, since some of the grain constituents may evaporate at the high temperatures (up to $\sim 10^3$ °K) mostly relevant here. If we suppose the dust grains to consist predominantly of graphite, then according to Hoyle & Wickramasinghe (1962) we would have $\kappa_\lambda \propto \lambda^{-2}$ for λ greater than about 1 μ.

(3) Scattering of radiation by the dust grains has been neglected, and only pure absorption and thermal emission have been considered. This is a good approximation at the long infra-red wavelengths, where scattering is negligible compared with absorption, but it is not a good approximation at visual wavelengths.

2. CALCULATION OF THE EMITTED SPECTRUM

We suppose for the moment that the temperature distribution in the cloud is known, and we consider the problem of calculating the total luminosity emitted at each wavelength. This involves integrating the contributions from all parts of the cloud, with an attenuation factor of the form $e^{-\tau}$ for each volume element and each line of sight. The result of this calculation can be written in the following form, analogous to the corresponding formula for a plane atmosphere:

$$L_\lambda = 16\pi^2 \int_0^\infty r^2(\tau_\lambda) G(\tau_\lambda) B_\lambda(\tau_\lambda)\, d\tau_\lambda, \tag{3}$$

where

$$\tau_\lambda = \int_r^\infty \kappa_\lambda \rho\, dr \tag{4}$$

and

$$G(\tau_\lambda) = \frac{1}{2r} \int_0^r \frac{s\, ds}{\sqrt{(r^2 - s^2)}} \left[\exp\left\{ -\int_s^\infty \kappa_\lambda \rho \frac{r\, dr}{\sqrt{(r^2 - s^2)}} - \int_s^r \kappa_\lambda \rho \frac{r\, dr}{\sqrt{(r^2 - s^2)}} \right\} + \exp\left\{ -\int_r^\infty \kappa_\lambda \rho \frac{r\, dr}{\sqrt{(r^2 - s^2)}} \right\} \right]. \tag{5}$$

In these equations L_λ is the luminosity emitted per unit wavelength interval, τ_λ is the radial optical depth at wavelength λ, and $B_\lambda(\tau_\lambda)$ is the blackbody radiation intensity function. The function $G(\tau_\lambda)$ has here been defined such that $G(0) = 1$. Clearly $G(\tau_\lambda)$ depends on the variation of $\kappa_\lambda \rho$ with r, and, therefore, it is not a ' universal function ' like the corresponding function $E_2(\tau_\lambda)$ for a plane atmosphere.

We shall define $G_n(\tau_\lambda)$ as the function obtained when equation (1) is substituted into equation (5). We have calculated the function $G_{3/2}(\tau_\lambda)$ numerically, and the result is tabulated in Appendix A. This tabulated function can then be used in conjunction with equation (3) to calculate the emitted spectrum L_λ, given the blackbody function $B_\lambda(\tau_\lambda)$ or equivalently the temperature distribution $T(\tau_\lambda)$.

3. THE TEMPERATURE DISTRIBUTION

In order to obtain an approximation for the temperature distribution in the infalling cloud, our procedure has been to construct a simple formula having the correct limiting forms at very small and very large optical depths. Considering first

the limit of small optical depths (i.e. large radii), it is easily shown that if the wavelength dependence of the absorption coefficient follows equation (2), then the dependence of temperature on radius is given by

$$T^4 = ar^{-8/(4+p)}, \tag{6}$$

where a is a constant depending on the emitted spectrum.

In the limit of large optical depths, the radiative transfer problem again simplifies greatly, and we can apply the radiation diffusion equation as used in the theory of stellar interiors:

$$L = -\frac{64\pi\sigma r^2 T^3}{3\kappa_R \rho}\frac{dT}{dr}, \tag{7}$$

where κ_R is the Rosseland mean opacity. For the absorption coefficient given in equation (2), the Rosseland mean is

$$\kappa_R = \frac{24\zeta(4)}{\Gamma(5-p)\zeta(4-p)}\left(\frac{T}{c_2}\right)^p \kappa_0, \tag{8}$$

where ζ is the Riemann zeta function and $c_2 = hc/k$. Since $\kappa_R \propto T^p$ and $\rho \propto r^{-n}$, it is convenient to set

$$\kappa_R \rho = KT^p r^{-n}. \tag{9}$$

Substituting equation (9) into equation (7), one can then solve for T as a function of r, using the boundary condition $T = 0$ at $r = \infty$. The result can be written

$$T^4 = \frac{3(n+p/2-1)}{(n+1)}\tau_R T_f^4, \tag{10}$$

where

$$\tau_R = \int_r^\infty \kappa_R \rho \, dr, \quad T_f^4 = \frac{L}{16\pi\sigma r^2}. \tag{11}$$

In deriving this result we have made use of the fact, as found in the dynamical calculations of Paper I, that the luminosity L is very nearly constant throughout the infalling cloud. The constancy of L results because the internal energy carried by the infalling material is negligible in comparison with the radiative energy flux.

The simplest way to construct an approximate formula for the temperature distribution at all optical depths is to add together the expressions for T^4 given in equations (6) and (10), which refer to the optically thin and optically thick limits respectively. The result, which is readily verified to be correct in these two limits, can be written

$$T = T_0 f(\tau_R), \tag{12}$$

where

$$T_0^4 = \left[\alpha^{-4}\beta^{-p}\left(\frac{2}{K}\right)^4\left(\frac{L}{16\pi\sigma}\right)^{2n-2}\right]^{\alpha/(4-p)} \tag{13}$$

and

$$f(\tau_R)^4 = \beta[A\tau_R^{-\alpha p/(4+p)} + \tau_R]\tau_R^{\alpha}. \tag{14}$$

Here τ_R is related to the optical depth τ_λ by

$$\tau_R = [C(\lambda T_0)^p \tau_\lambda]^{\gamma/\alpha}, \tag{15}$$

where

$$C = \frac{\alpha}{\gamma}\beta^{p/4}\frac{24\zeta(4)}{\Gamma(5-p)\zeta(4-p)c_2{}^p}. \tag{16}$$

In these equations the constants α, β, and γ are defined by

$$\alpha = \frac{4-p}{2n+p-2}, \quad \beta = \frac{3(n+p/2-1)}{n+1}, \quad \gamma = \frac{2}{n-1}. \tag{17}$$

We still have one undetermined parameter, namely the constant A in equation (14), which is related to the constant a in equation (6). We have arbitrarily chosen this parameter such as to satisfy the condition that the resulting spectrum must give the correct total luminosity L when integrated over all wavelengths. With $n = 3/2$, the values of A determined in this way for $p = 1$, $3/2$, and 2 are 0·831, 0·645, and 0·354, respectively.

When the above procedure for obtaining a simple approximation to the temperature distribution is applied in the grey case ($p = 0$, $\tau_R = \tau_\lambda = \tau$), the result is

$$T^4 = \left[1 + \frac{3(n-1)}{(n+1)}\tau\right] T_f^4. \tag{18}$$

In this case there is no undetermined parameter A. This form for the temperature distribution in the grey case is supported by the work of Chapman (1966), who studied the special case $n = 3$. For $n = 3$ our approximation becomes

$$T^4 = (1 + \tfrac{3}{2}\tau)T_f^4,$$

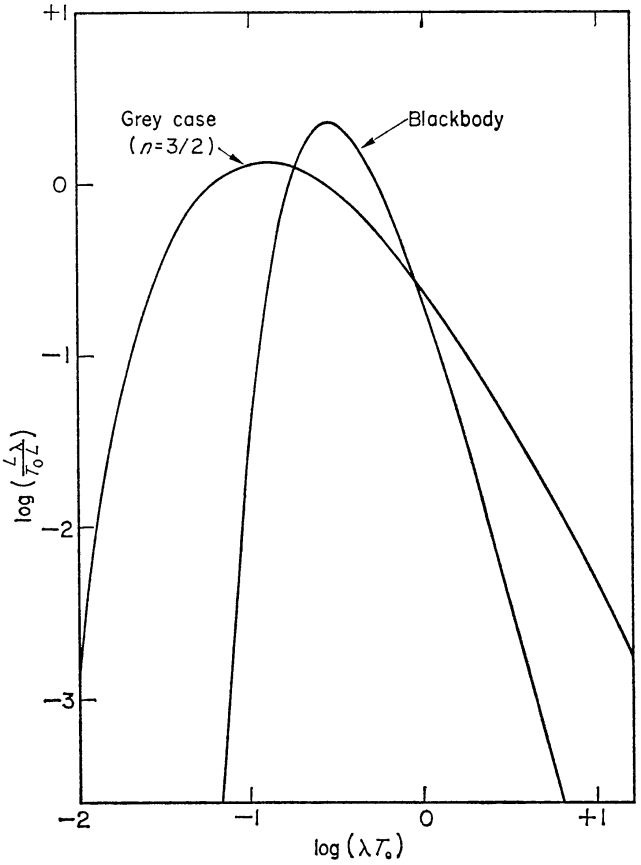

FIG. 1. *The emitted spectrum of a proto-stellar cloud with $n = 3/2$ and $p = 0$ (grey case). A blackbody spectrum of temperature T_0 is also shown for comparison. Both curves are normalized to unity when integrated with respect to the independent variable λT_0. All units are CGS units.*

whereas Chapman's approximation, based on some detailed calculations of the radiation field, is equivalent to

$$T^4 = (1{\cdot}154 + \tfrac{3}{2}\tau)T_f{}^4.$$

It may be noted that our approximation is correct at small optical depths, whereas Chapman's is not.

4. RESULTS FOR THE EMITTED SPECTRUM

If we now substitute equation (12) along with the blackbody radiation law into equation (3), the resulting expression for L_λ can be written

$$L_\lambda = C^{-\gamma}\frac{c_1}{\sigma}\frac{T_0 L}{(\lambda T_0)^{5+\gamma p}}\int_0^\infty \frac{\tau_\lambda{}^{-\gamma} G_n(\tau_\lambda)\, d\tau_\lambda}{\exp\{c_2/\lambda T_0 f(\tau_R)\} - 1}, \tag{19}$$

where $c_1 = 2\pi hc^2$. It is evident from equations (19) and (15) that L_λ depends on λ only in combination with T_0 in the factor (λT_0); therefore, it is convenient to consider λT_0 as the independent variable and calculate L_λ as a function of λT_0. Also it is convenient to calculate not L_λ itself but $L_\lambda/T_0 L$; the resulting function is then independent of the parameters L and T_0, and is normalized to unity when integrated with respect to the independent variable λT_0.

Some of the resulting spectra calculated numerically from equation (19) are illustrated in Figs 1 and 2. Fig. 1 shows the spectrum for $n = 3/2$ and $p = 0$ (the

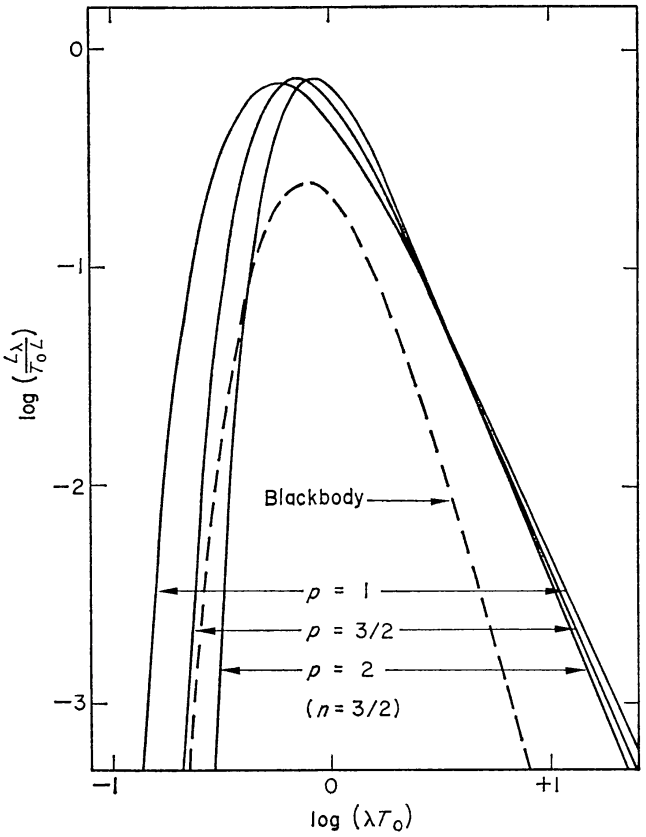

FIG. 2. *The emitted spectrum of a proto-stellar cloud with* $n = 3/2$ *for the three cases* $p = 1$, $p = 3/2$, *and* $p = 2$. *The curves are normalized when integrated with respect to* λT_0. *The blackbody spectrum (dashed curve) has been arbitrarily positioned on the diagram for purposes of comparison.*

grey case), and Fig. 2 shows the results for $p = 1$, $3/2$, and 2. It is evident in these diagrams that the grey spectrum is very much broader than a blackbody spectrum, and that the emitted spectrum becomes much narrower as p is increased. The reason for this is that the radiation at the shorter wavelengths, which comes mainly from the hotter inner parts of the cloud, is selectively absorbed to a greater and greater extent with increasing p because of the increase in κ_λ toward shorter wavelengths; at the same time, there is less long wavelength radiation from the cooler outer parts of the cloud, owing to the reduced opacity and, hence, the reduced emission at the longer wavelengths. It is evident from Figs 1 and 2 that these effects are quite large, and it appears that the grey case is inadequate even as a rough approximation in the present problem.

We are now in a position to predict the spectrum of a spherically symmetric proto-star at any time in its evolution, assuming that the opacity of the dust grains can be represented by a formula of the form $\kappa_\lambda = \kappa_0 \lambda^{-p}$ and that suitable values for κ_0 and p can be estimated. For purposes of illustration we have adopted $p = 3/2$, and we have obtained κ_0 by fitting to the interstellar extinction curves of van de Hulst (1949) at near infrared wavelengths. The resulting opacity law is

$$\kappa_\lambda = 7 \times 10^{-5} \lambda^{-3/2} \text{ cm}^2 \text{ g}^{-1}. \tag{20}$$

As we have noted, the shape of the emitted spectrum remains constant as the proto-star evolves, and only the parameters L and T_0 vary. The luminosity L is known from the dynamical calculations of Paper I, and the parameter T_0 depends through equations (13), (9), and (8) on L and also on the density of the infalling material, which again is known from the dynamical calculations. The parameter T_0 determines the wavelength λ_{max} at which L_λ is a maximum; as T_0 increases, λ_{max} decreases, the product $\lambda_{max} T_0$ remaining constant. We can conveniently present the results for the variation in spectral appearance of the proto-star in a diagram

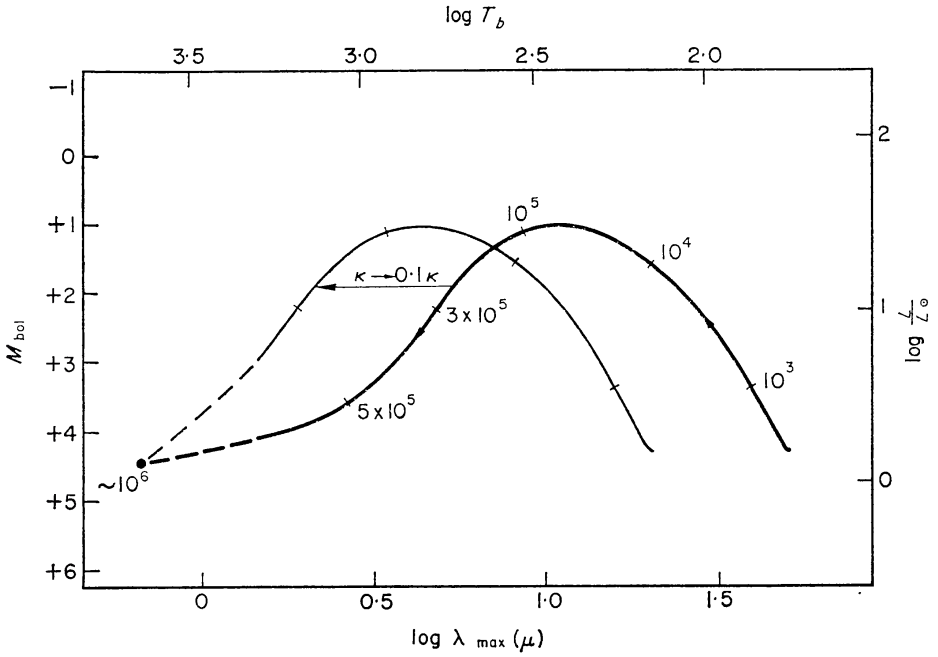

FIG. 3. *The evolution in spectral appearance of a proto-star in Case* 1 (*heavy curve*), *corresponding to Fig.* 3 *of Paper I for the evolution of the stellar core. The numbers marked along the curve are the times in years since the formation of the stellar core. The lighter curve and the arrow marked* '$\kappa \rightarrow 0{\cdot}1\,\kappa$' *show the effect of reducing the dust opacity by a factor of* 10.

analogous to the HR diagram, in which we plot L vs. λ_{max} for the proto-star as it evolves. This has been done in Figs 3–5 for several of the cases calculated in Paper I. In these diagrams we have added a scale giving the ' apparent blackbody temperature ' T_b defined by $\lambda_{max} T_b = 0{\cdot}29$ cm °K.

Fig. 3 shows the results for Case 1 of Paper I, which was calculated for a proto-star of one solar mass using what were thought to be the best values of all parameters. It is seen that λ_{max} decreases continually during the evolution, while L first increases and then decreases again. The reason for the steady decrease in λ_{max} is that as the collapse proceeds and the density of the infalling material decreases, optical depth unity in the collapsing cloud occurs at smaller and smaller radii and hence at higher and higher temperatures. Since the dust opacity may be considerably less than we have assumed, owing to evaporation of some of the grain constituents, we have shown in Fig. 3 the effect of reducing the opacity by a factor of 10; this shifts the whole curve to the left (smaller λ_{max}) by 0·4 in log λ_{max}.

In the innermost part of the collapsing cloud, the temperature is high enough to evaporate the dust grains completely; thus there is no absorption inside the point where the grains evaporate. When the density of the infalling material becomes so low that the optical depth of the cloud becomes of the order of unity or less, the central stellar object starts to become visible, and the spectrum no longer has the shape which we have calculated. If the dust evaporation temperature is taken to be ~ 2000 °K, this occurs when $\lambda_{max} \sim 1{\cdot}5\ \mu$; this point is indicated in Fig. 3 by the transition from a solid curve to a dashed curve. The spectrum of the proto-star during the final phase of evolution will be discussed in the following section.

Fig. 4 shows the evolution in spectral appearance for Case 2 of Paper I, which was calculated again for one solar mass but with a much higher initial temperature and density than Case 1. The shape of the curve in Case 2 is much the same as in Case 1, but it is shifted to higher luminosities and longer wavelengths because of the higher density of the infalling material. The results for Case 6 ($M = 2M_\odot$) and Case 7 ($M = M_\odot$) are shown in Fig. 5. Case 6 is again qualitatively similar to Cases

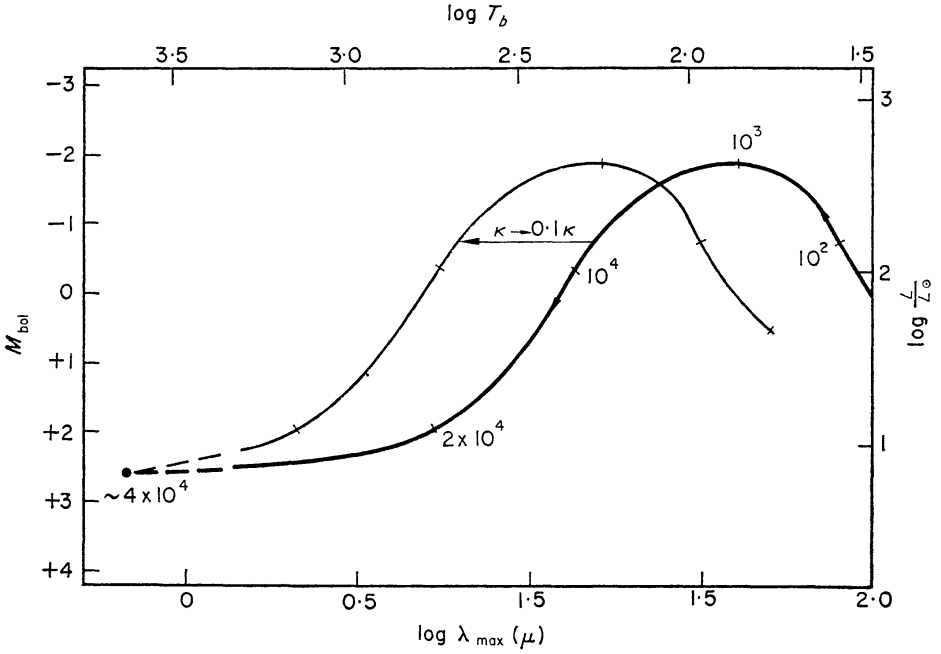

FIG. 4. *The evolution in spectral appearance of the proto-star in Case 2.*

1 and 2, but Case 7 differs during the later stages of the evolution because the luminosity is then supplied by radiative cooling of the stellar core and no longer as in the other cases by the kinetic energy inflow to the core.

In Figs 3–5 the final point on the curve represents in each case the position in the HR diagram of the star finally resulting at the end of the dynamical collapse phase. As was mentioned in Paper I, these points tend to fall near the lower end of the conventional 'Hayashi track' for the convective phase of pre-main-sequence evolution, and they are in good general agreement with the observed positions of T Tauri stars in the HR diagram. In Case 7 ($M = 5M_\odot$) a convective 'Hayashi' phase is never reached and when the star first becomes visible, it is already considerably closer to the main sequence than the lower end of the Hayashi track.

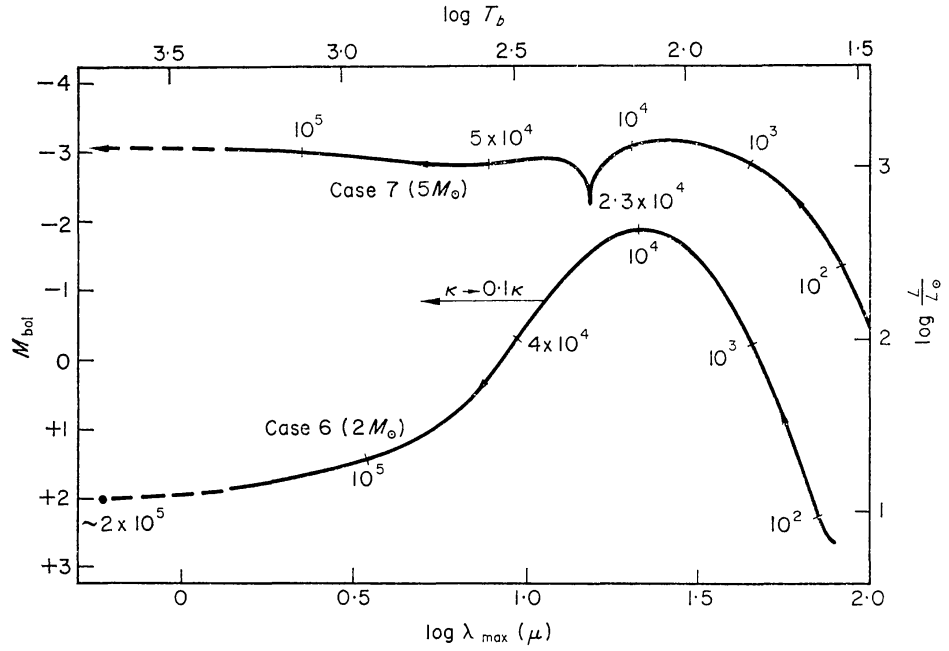

FIG. 5. *The evolution in spectral appearance of the proto-star in Case* 6 ($M = 2\,M_\odot$) *and Case* 7 ($M = 5\,M_\odot$).

5. FINAL STAGES OF THE EVOLUTION

When the infalling material is no longer completely optically thick, the emitted spectrum of the proto-star consists of two components: (1) the radiation from the central stellar core, still attenuated by the dust in the infalling material, and (2) the thermal infrared emission from the dust. For purposes of illustration, we have represented the spectrum of the stellar core by a blackbody spectrum. The thermal emission from the dust has been calculated as before from equation (19), taking the upper limit on the integral to be the optical depth at the point where the grains evaporate. We have again adopted $p = 3/2$, and we have assumed that the opacity law $\kappa_\lambda = \kappa_0\lambda^{-p}$ holds even at visual wavelengths. The resultant spectrum has been calculated in approximately normalized form from the formula

$$\frac{L_\lambda}{L} = \exp(-\tau_\lambda)\frac{B_\lambda(T_s)}{B(T_s)} + \frac{L_\lambda(\tau_\lambda)}{L}, \tag{21}$$

where τ_λ is the optical depth at the point where the grains evaporate and T_s is the

temperature of the (blackbody) stellar spectrum. $L_\lambda(\tau_\lambda)$ is the dust emission spectrum as calculated from equation (19) with the integral cut off at optical depth τ_λ.

For purposes of illustration, we have adopted $T_s = 5000\,°\mathrm{K}$ and a dust evaporation temperature of 1000 °K, and we have calculated the resultant spectrum for several different values of the total optical depth of the cloud. The resulting family of curves is illustrated in Fig. 6. The emergence of the stellar spectrum and the decrease of the dust emission component with decreasing optical depth are evident. In Case 1 the time scale for these changes is such that the time interval between adjacent curves in Fig. 6 is about 4×10^4 years. Clearly, there is a wide range of possibilities for the resultant spectrum if different values for T_s and the dust evaporation temperature are considered.

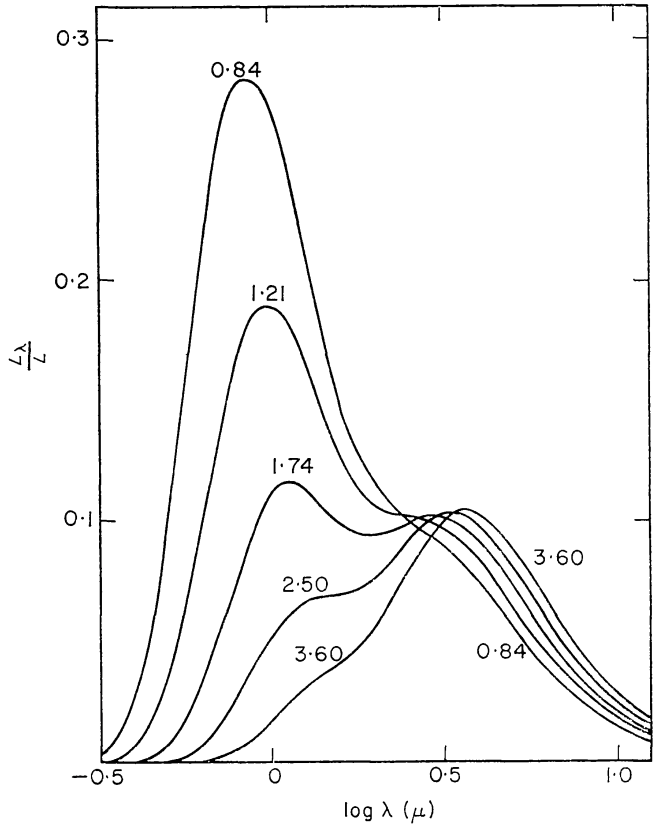

FIG. 6. *The emitted spectrum of a proto-star when the infalling cloud is no longer completely optically thick, calculated for a core temperature of* 5000 °*K and a dust evaporation temperature of* 1000 °*K. The curves shown are approximately normalized, and are labelled with the optical depth of the cloud at a wavelength of* 1 *micron.*

6. COMPARISON WITH OBSERVATION

(a) *Infrared observations in Orion*

Becklin & Neugebauer (1967) have reported observations of an infra-red point source in the Orion nebula which they think may be a proto-star. The infra-red flux measurements for this object are plotted vs. wavelength in Fig. 7. It is not known to what extent the observations may be affected by interstellar extinction, but qualitatively the appearance of the object is much the same as would be predicted for a proto-star during the phase when the infalling cloud is still optically thick. The inferred luminosity ($\sim 10^3\,L_\odot$) and the apparent blackbody temperature ($\sim 700\,°\mathrm{K}$)

of this object are within the range of our results for evolving proto-stars (see for example Fig. 5). If the Becklin–Neugebauer object is interpreted as a proto-star, it appears that it must have a mass greater than 1 $M_\odot$, perhaps more like 5 $M_\odot$.

In Fig. 7 the observations of Becklin & Neugebauer (filled circles with error bars) have been fitted as well as possible with a blackbody spectrum (dashed curve) and with the best fitting curve from among those plotted in Fig. 2, which turns out to be the one for $p = 2$, as would be appropriate, for example, for graphite dust grains. The 5 μ measurement of Kleinmann & Low (1967) is not fitted by any of the calculated curves. Because of the unknown dust absorption properties and the very idealized nature of our model, however, one should probably not expect better than qualitative agreement in a comparison of this kind.

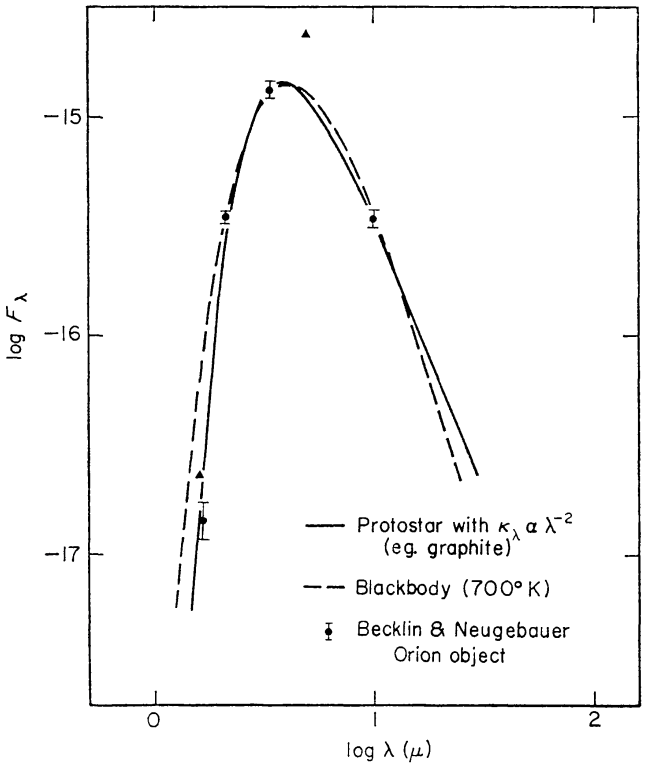

FIG. 7. *Infra-red flux measurements of the Becklin–Neugebauer object in Orion. The filled circles with error bars are the observations of Becklin & Neugebauer* (1967), *and the triangles are the observations of Kleinmann & Low* (1967). *The unit of* F_λ *is* $W\ cm^{-2}\ \mu^{-1}$. *See text for explanation of the curves.*

Kleinmann & Low (1967) have reported observation of an extended infra-red nebula near the Becklin–Neugebauer point source in Orion. This extended nebula apparently radiates most of its energy at much longer wavelengths than the Becklin–Neugebauer object, and is inferred with considerable uncertainty to have a linear diameter of $\sim 2 \times 10^{17}$ cm, a luminosity of $\approx 10^5\ L_\odot$, and an 'effective temperature' of ≈ 70°K. Hartmann (1967) has interpreted this object as an opaque dust cloud, whose luminosity is supplied by a group of massive newly formed stars imbedded in it. A similar idea has also been proposed by Davidson & Harwit (1967). This is qualitatively the same kind of situation which is predicted by our calculations of star formation. Our calculations are probably not directly applicable to this

object, however, since it appears that the formation of a multiple system or at least a single very massive star may be involved.

(b) *Infra-red observations of T Tauri stars*

Mendoza (1966, 1968) has made wide-band photometric observations of T Tauri stars over a wavelength range from 0·36 to 5 μ. Nearly all of these stars show considerable excess infra-red emission relative to a normal stellar spectrum, sometimes to the extent that nearly all of the energy is emitted in the infra-red, as is the case for example with R Mon. Qualitatively, this is just what would be predicted if we interpret the T Tauri stars as newly formed stars still surrounded by some remaining proto-stellar material, which absorbs part of the stellar radiation and re-emits it at infra-red wavelengths.

Unfortunately, since T Tauri stars vary irregularly and since Mendoza's observations were not made simultaneously at all wavelengths, Mendoza's data do not in most cases yield reliable spectral energy distributions for these stars. It is clear, however, that there are wide variations from star to star; also, it appears in general that the infra-red emission is more widely distributed in wavelength than would be predicted from our calculations, as illustrated for example in Fig. 6. This is probably to be expected, however, because of the idealized nature of our model for the infalling cloud; if the cloud has inhomogeneities or deviations from spherical symmetry, or if the dust grains or grain constituents do not all evaporate at the same temperature, then one would in general expect the emitted spectrum to contain significant contributions from a wider range of temperatures than is the case in our simple model.

ACKNOWLEDGMENTS

I am indebted to Dr G. Münch for several helpful discussions. The work reported here has been supported in part through NSF grant GP-7030.

Mount Wilson and Palomar Observatories, Carnegie Institution of Washington, California Institute of Technology.

Present address:
Yale University Observatory, New Haven, Connecticut 06520.

REFERENCES

Becklin, E. E., & Neugebauer, G., 1967. *Astrophys. J.*, **147**, 799.
Chapman, R. D., 1966. *Astrophys. J.*, **143**, 61.
Davidson, K., & Harwit, M., 1967. *Astrophys. J.*, **148**, 443.
Hartmann, W. K., 1967. *Astrophys. J.* (*Letters*), **149**, L87.
Hoyle, F., & Wickramasinghe, N. C., 1962. *Mon. Not. R. astr. Soc.*, **124**, 417.
Johnson, H. L., 1965. *Astrophys. J.*, **141**, 923.
Johnson, H. L., & Borgmann, J., 1963. *Bull. astr. Inst. Netherl.*, **17**, 115.
Kleinmann, D. E., & Low, F. J., 1967. *Astrophys. J.* (*Letters*), **149**, L1.
Larson, R. B., 1969. *Mon. Not. R. astr. Soc.*, **145**, 271.
Mendoza, E. E., 1966. *Astrophys. J.*, **143**, 1010.
Mendoza, E. E., 1968. *Astrophys. J.*, **151**, 977.
Van de Hulst, H. C., 1949. *Rech. astr. Obs. Utrecht*, **11**, Part 2.

APPENDIX A

CALCULATION OF THE FUNCTION $G_{3/2}(\tau_\lambda)$

As mentioned previously, the functions $G_n(\tau_\lambda)$ are defined by substituting equation (1) into equation (5). If we make this substitution for $n = 3/2$, and then employ the transformation of variables $r = s \sec^2 \phi$, the resulting expression for $G_{3/2}(\tau_\lambda)$ reduces to

$$G_{3/2}(\tau_\lambda) = \int_{-\pi/2}^{\pi/2} \frac{\cos^3 \phi \, d\phi}{\sqrt{(1+\cos^2 \phi)}} \exp\left\{\frac{\tau_\lambda}{\sqrt{2}\cos\phi}\left[F\left(\frac{1}{\sqrt{2}}, \phi\right) - F\left(\frac{1}{\sqrt{2}}, \frac{\pi}{2}\right)\right]\right\}, \quad \text{(A 1)}$$

where $F(k, \phi)$ is the Elliptic Integral of the First Kind. Here we have made use of the relation $\tau_\lambda = 2K_\lambda r^{-1/2}$ valid for $n = 3/2$. We have used equation (A 1) to calculate the function $G_{3/2}(\lambda_\lambda)$ by numerical quadrature, using a subroutine available at the Caltech computing centre to evaluate the elliptic integrals. Some values of $G_{3/2}(\tau_\lambda)$ obtained in this way are listed in Table AI.

TABLE AI

τ_λ	$G_{3/2}(\tau_\lambda)$	τ_λ	$G_{3/2}(\tau_\lambda)$	τ_λ	$G_{3/2}(\tau_\lambda)$
0·0	1·000	1·0	2·459(−1)	3·4	1·313(−2)
0·1	8·573(−1)	1·2	1·897(−1)	3·8	8·257(−3)
0·2	7·385(−1)	1·4	1·470(−1)	4·2	5·213(−3)
0·3	6·385(−1)	1·6	1·143(−1)	4·6	3·303(−3)
0·4	5·538(−1)	1·8	8·911(−2)	5·0	2·100(−3)
0·5	4·815(−1)	2·0	6·967(−2)	5·8	8·555(−4)
0·6	4·195(−1)	2·2	5·460(−2)	6·6	3·517(−4)
0·7	3·662(−1)	2·4	4·288(−2)	7·4	1·457(−4)
0·8	3·202(−1)	2·6	3·374(−2)	8·2	6·074(−5)
0·9	2·804(−1)	3·0	2·099(−2)	9·0	2·546(−5)